The AIB1siRNA-loaded hyaluronic acid-assembled PEI/heparin/Ca²⁺ nanocomplex as a novel therapeutic strategy in lung cancer treatment

YING HAO[1], YONGSHENG GAO[2], YEDAN WU[3] and CHANGSHAN AN[3]

[1]Department of Pathology, Key Laboratory of Xinjiang Endemic and Ethnic Diseases, Ministry of Education, Shihezi University School of Medicine, Shihezi, Xinjiang 832003; [2]Department of Pathology, Shandong Cancer Hospital Affiliated to Shandong University, Jinan, Shandong 250117; [3]Department of Respiratory Medicine, Yanbian University Hospital, Yanji, Jilin 133000, P.R. China

Abstract. In the present study, AIB1siRNA-loaded polyethyleneimine (PEI)/heparin/Ca²⁺ nanoparticles (NPs) were successfully prepared and evaluated for their efficacy in lung cancer cells. The results demonstrated that the PEI and heparin complex reduced the toxic effect in cancer cells while maintaining its transfection efficiency. A nanosized particle of ~25 nm was formulated and siRNA was demonstrated to possess excellent binding efficiency in the particles. Confocal microscopy revealed that fluorescein-labeled (FAM)-small interfering (si) RNA dissociated from the HA-PEI/heparin/Ca²⁺/siRNA (CPH-siH) NPs and exhibited maximum fluorescence in the cytoplasm, which was important in elucidating its post-transcriptional activity. CPH-siH NPs exhibited a typical concentration-dependent toxicity in cancer cells. Blank PEI/heparin/Ca²⁺ did not induce any toxicity in cancer cells, indicating its safety and lack of side effects. CPH-siH (100 nm) induced the maximum apoptosis of cancer cells with nearly ~35% of cells in the early and late apoptosis stages. The expression of the nuclear receptor coactivator 3 (NCOA3, also known as AIB1) protein was knocked down in a concentration-dependent manner, demonstrating the potent activity of AIB1siRNA in cancer cells. Together, these results indicated that HA-PEI/heparin/Ca²⁺ NPs may be a promising carrier for the anticancer activity of AIB1siRNA in lung cancer cells.

Correspondence to: Dr Yongsheng Gao, Department of Pathology, Shandong Cancer Hospital Affiliated to Shandong University, 440 Jiyan Road, Jinan, Shandong 250117, P.R. China
E-mail: guttecheliha@yahoo.com

Introduction

Lung cancer is one of the leading causes of cancer-related death in both men and women, worldwide (1). Histologically, two different types of lung cancer exist, which are classified based on their microscopic appearance (2). Among these two types, non-small cell lung cancer (NSCLC) represents 85-90% of lung cancers (3). Most patients diagnosed with NSCLC have advanced-stage disease and have a mean 5-year survival of 17.4% (4). Various strategies are currently used to treat NSCLC, including radiotherapy, chemotherapy, surgery, and monoclonal antibodies; however, there is no single therapy that is reliable and successful (5,6).

Gene therapy is emerging as an alternative to conventional therapy, which has been associated with adverse effects during cancer treatment (7). Gene therapy involves the insertion of genetic material into cancer cells, which modifies gene expression during cancer management (8,9). In the present study, the oncogene nuclear receptor coactivator 3 (NCOA3, also known as AIB1) was selected as a target. AIB1 is a member of the p160 steroid receptor coactivator family (10). It is widely expressed in many types of cancer, including high expression in lung cancer cells, and it has been reported that the expression levels of AIB1 are directly associated with patient survival (11). AIB1 is strongly associated with apoptosis, tumorigenesis, and cancer metastasis (12). Therefore, it was hypothesized that knockdown of AIB1 may result in increased therapeutic efficacy in lung cancers.

One of the important aspects of gene therapy is the efficient delivery of the gene to the target cells without any side effects to major organs. Ideally, the gene delivery system should be target-specific, nontoxic, biocompatible, and stable during storage conditions (13,14). Non-viral polymer carriers are considered to be more beneficial than viral gene carriers because of the reduced risk of an immune response. Polyethyleneimine (PEI) is one of the most used and tested cationic carriers for gene delivery (15). PEI is known to possess high transfection efficiency both *in vitro* and *in vivo* (16). However, branched PEI has been associated with a high risk of toxicity compared with viral vectors (17). To reduce the toxicity of PEI, while at the

same time maintaining its transfection efficiency, heparin is used, which is a negatively charged anticoagulation agent (18). Heparin is biocompatible and widely used in clinical studies. Furthermore, the high negative charge of heparin allows a strong physical interaction with its cationic counterparts (19). Several studies of the heparin and protamine sulphate complex have reported that it is associated with significantly increased intracellular delivery (20,21). In the present study, a nano-complex based on PEI/heparin in the presence of Ca^{2+} ions was produced to form intact particles. To protect the siRNA in the systemic circulation, a protective layer around the PEI/heparin/Ca^{2+} particles was also assembled. Hyaluronic acid (HA) is a natural polysaccharide, which is present in abundance in the extracellular matrix and synovial fluids of the body. The negatively charged HA forms a layer around the positively charged PEI/heparin/Ca^{2+} particles to maximize its stability. In addition, HA acts as a targeting agent by forming a receptor complex with CD44 receptors in cancer cells (22).

The major objective of the present study was to deliver AIB1 small interfering (si)RNA into lung cancer cells. For this purpose, siRNA was loaded in PEI/heparin/Ca^{2+} nanoparticles (NPs), then coated with HA as a protective layer. The efficiency of the HA-PEI/heparin/Ca^{2+}/siRNA (CPH-siH) was then evaluated using cell viability, cell apoptosis, and western blot protein expression analyses.

Materials and methods

Reagents. Heparin sodium, calcium chloride, and HA were purchased from Sigma-Aldrich (Merck KGaA, Darmstadt, Germany). Branched PEI (25 kDa) was also purchased from Sigma-Aldrich (Merck KGaA). The sequences of siAIB1 were 5'-r(GGUGAAUCGAGACGGAAAC)dTT-3' and 5'-r(GUU UCCGUCUCGAUUCACC)dTTT-3'. All other chemicals were of reagent grade.

Preparation of HA-assembled AIB1siRNA-loaded PEI/heparin/Ca^{2+} NPs. A synthetic route was used to prepare HA-PEI/heparin/Ca^2/siRNA (CPH-siH). A total of 2 ml of $CaCl_2$ solution (22 mg/ml), 1 ml of PEI (32 mg/ml), and 0.5 ml of heparin (32 mg/ml) was mixed together and stirred for 45 min at 800 rpm/min. The volume was increased to 50 ml and further stirred for 20 h. At the end of this period, a white-colored precipitate was formed, which was collected by centrifuging at 3,000 x g for 15 min. The particle was washed three times until all the unreacted initial components were removed. The resulting PEI/heparin/Ca^{2+} was dispersed in 1 ml of saline, and siRNA was added and further incubated for 12 h at 4˚C. The resulting PEI/heparin/Ca^2/siRNA was collected by centrifugation at 1,400 x g for 5 min. HA solution at a weight ratio of 5:1 (siRNA complex:HA) was added and gently stirred for 30 min. Finally, NPs were centrifuged at 250 x g for 10 min and the pellet was resuspended in ultrapure water and stored at 4-8˚C.

Gel retardation assay. The loading of siRNA into particles was evaluated by agarose gel electrophoresis. The CPH-siH and siRNA were mixed in different NP ratios, and the preparation was analyzed as previously mentioned. A 1% agarose gel was prepared and prestained with 0.5 mg/ml of ethidium bromide. The agarose gel was loaded with different samples and run at 100 V in Tris-acetate buffer (0.001 M EDTA). The bands formed in the gel were evaluated using an UltraLum Electronic UV Transilluminator (300 nm) with a Cohu High Performance Monochrome CCD Camera (Rose Scientific, Edmonton, Canada).

Particle size and surface charge analysis. The particle size was determined by dynamic light scattering (DLS) using a Zetasizer ZS (Malvern, Worcestershire, UK) at 25˚C. The zeta potential was measured using electrophoretic cells. The samples were appropriately diluted, and the experiments were conducted in triplicate.

Morphology. The morphology of the particles was visualized by transmission electron microscopy (SM-2000EX; JEOL, Tokyo, Japan) at an accelerating voltage of 120 kV. The particles were suitably diluted and placed in a copper grid and stained with 2% phosphotungstic acid as a negative stain. The grid was air dried and then visualized.

Cellular distribution. The cellular distribution of CPH-siH in A549 cancer cells (American Type Culture Collection, Manassas, VA, USA) was evaluated by confocal laser scanning microscopy (CLSM). Briefly, $2x10^5$ cells were seeded into 6-well plates and incubated for 24 h. The medium was removed the next day and the cells were treated with CPH-siH. For this purpose, fluorescein-labeled (FAM)-siRNA was used and loaded in the CPH-siH. After 2 h of incubation, the cells were carefully washed with PBS and fixed with 4% paraformaldehyde for 10 min. The cells were then washed again and stained with DAPI stain for 10 min. The cells were washed three times with PBS to remove all of the unbound DAPI, and observed (magnification, x40) using CLSM with 4 fields of view for each sample.

Cell viability assay. The effect of CPH-siH on the viability of A549 lung cancer cells was evaluated using the MTT assay. Briefly, $1x10^4$ cells were seeded into 96-well plates and incubated for 24 h. The medium was removed the next day and treated with different concentrations of CPH-siH and further incubated for 24 h. As a control, cells were incubated with blank NPs in parallel. Following the 24 h incubation, the medium was carefully removed and the cells were washed twice with PBS. The cells were then treated with 100 μl MTT solution (1.25 mg/ml) and incubated for 4 h, followed by the addition of 100 μl of dimethyl sulfoxide. After 15 min, the cells were shaken in a shaker, and the absorbance was measured using a microplate reader at 570 nm.

Apoptosis assay. To evaluate the mechanism of cell death, an apoptosis assay was performed using Annexin V/propidium iodide (PI) (BD Biosciences, Franklin Lakes, NJ, USA) staining and flow cytometry. Briefly, $2x10^5$ cells were seeded into 12-well plates and incubated for 24 h. The medium was removed the next day and treated with different concentrations of CPH-siH for 24 h. The next day, the medium was carefully removed and the cells were detached using a cell scraper (VWR International, Radnor, PA, USA). The cells were then centrifuged and the pellet was resuspended in 100 μl PBS and stained with 5 μl Annexin V-fluorescein isothiocyanate and
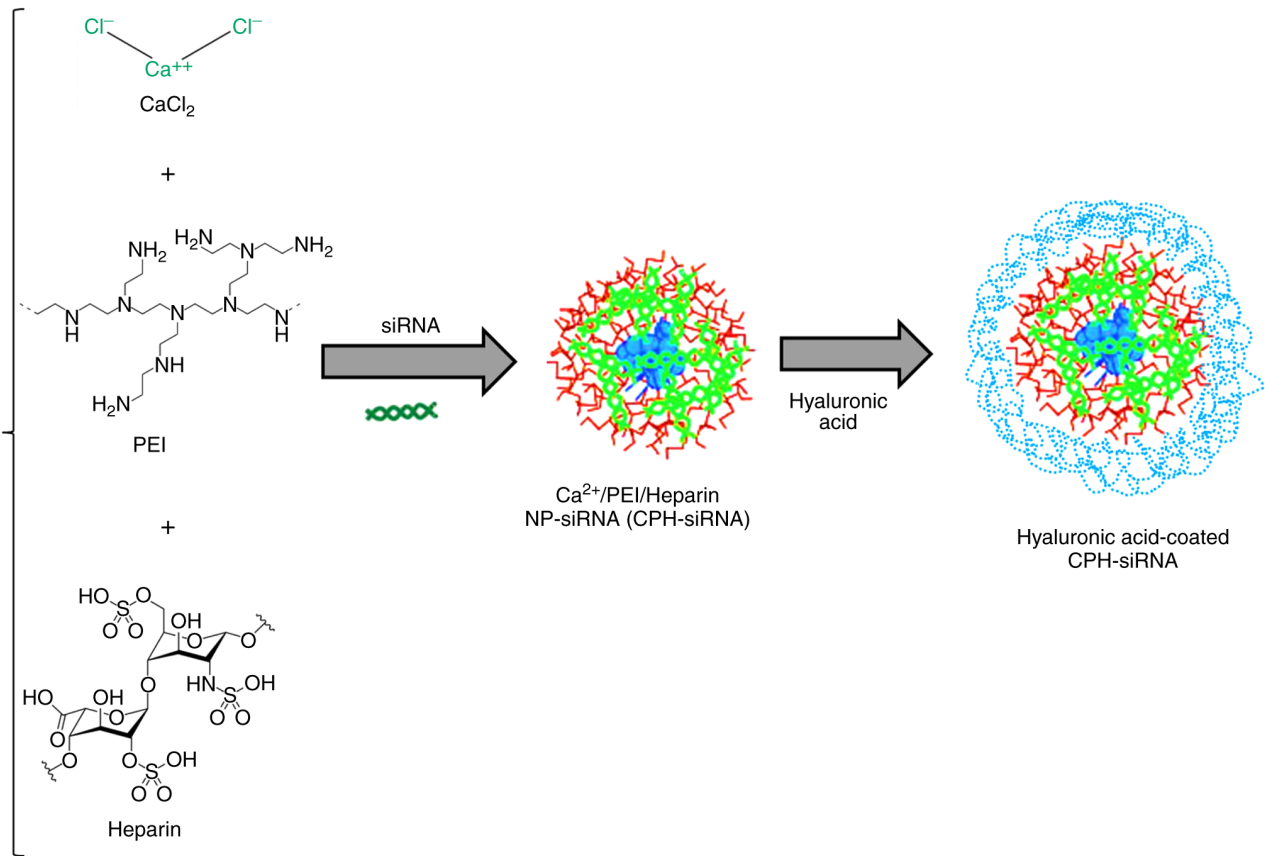
Figure 1. Schematic presentation of the siRNA-loaded PEI/Heparin/Ca^{2+}-HA nanoparticle preparation. The electrostatically assembled PEI/Heparin/Ca^{2+} was coated with HA as a protective cover. siRNA, small interfering RNA; PEI, polyethyleneimine; HA, hyaluronic acid.
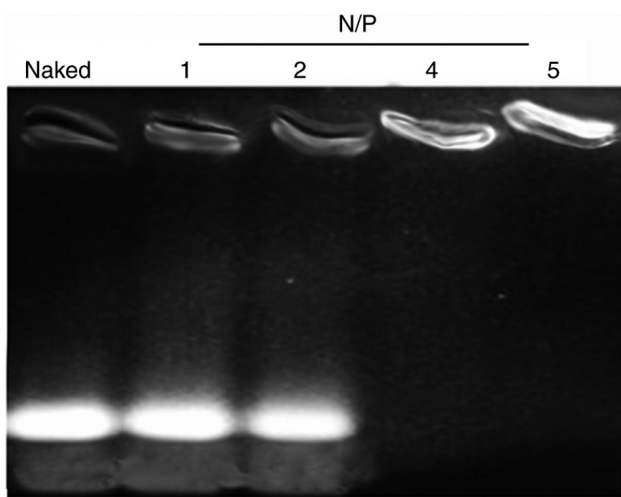
Figure 2. Binding efficiency of siRNA with PEI/Heparin/Ca^{2+}-HA, as determined by gel electrophoresis. Various N/P ratios of siRNA to PEI/Heparin/Ca^{2+}-HA were tested. siRNA, small interfering RNA; PEI, polyethyleneimine; HA, hyaluronic acid; N/P, nitrogen/phosphate.

5 μl PI for 15 min. The volume was made up to 1,000 μl and the cells were analyzed using a flow cytometer (BD FACS; BD Biosciences). Data analysis was performed using FlowJo software (version 8.6.6; Tree Star, Inc., Ashland, OR, USA).

Western blot analysis. The effect of the AIB1siRNA was examined by western blot analysis. Briefly, 3x10^5 cells were seeded into 6-well plates and incubated for 24 h. The medium was removed the next day and treated with different concentrations of CPH-siH for 24 h. Then, the medium was carefully removed and the cells were detached using a scraper. The cells were lysed using a lysis buffer (Cell Signaling Technology, Inc., Danvers, MA, USA) and centrifuged at 3,500 x g for 15 min. The supernatant was collected and its protein concentration was determined using Bradford assay protocol. The sample was solubilized with Laemmli buffer, and the proteins were separated by 10% SDS-PAGE, followed by transferring to polyvinylidene difluoride membranes (Pall Life Sciences, Port Washington, NY, USA). The membrane was blocked with 5% non-fat milk at 24°C for 1 h and incubated with mouse primary antibodies targeting AIB1 (Thermo Fisher Scientific, Inc., Waltham, MA, USA; MA5-15898; 1:1,000), Bcl-2 (SC-7382; 1:1,000), or GAPDH (SC-25778; 1:2,000; both Santa Cruz Biotechnology, Inc., Dallas, TX, USA) overnight at 4°C. The next day, the membranes were washed three times with Tris-buffered saline/0.1% Tween-20 (TBST) and incubated with horseradish peroxidase-conjugated mouse secondary antibodies (7076; 1:3,000; Santa Cruz Biotechnology, Inc.) for 1 h at room temperature. The blots were washed again with TBST and the bands were visualized with chemiluminescence detection reagent (Pierce; Thermo Fisher Scientific, Inc.), as per the manufacturer's instructions.

Statistical analysis. Statistical significance was determined by one-way analysis of variance with Tukey's adjustment for
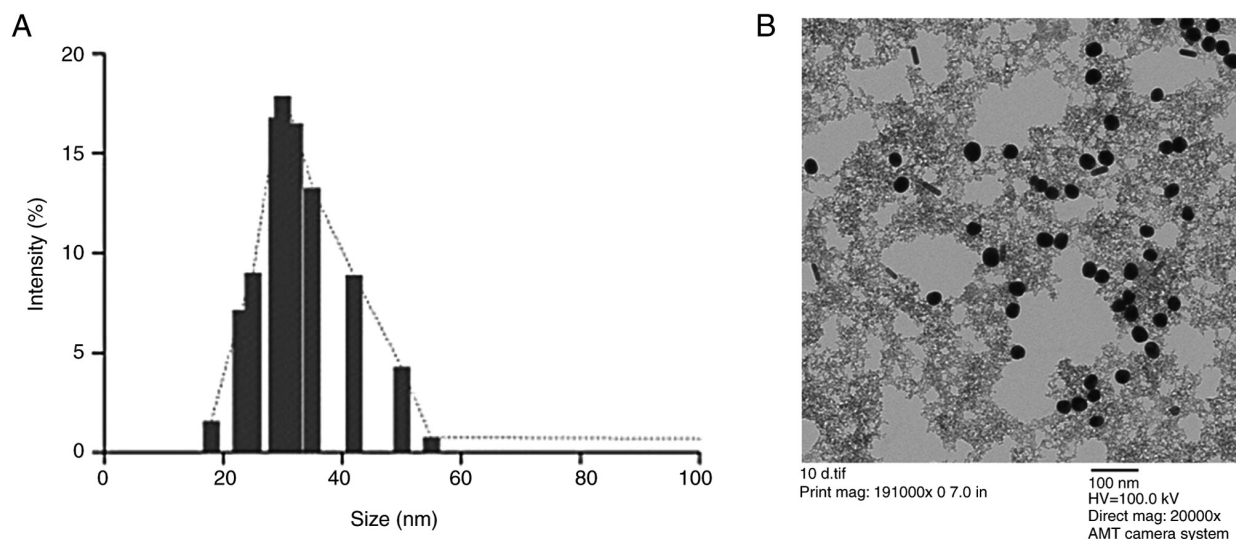
Figure 3. Particle characteristics. (A) Particle size analysis using dynamic light scattering. (B) Particle morphology analysis by transmission electron microscopy.
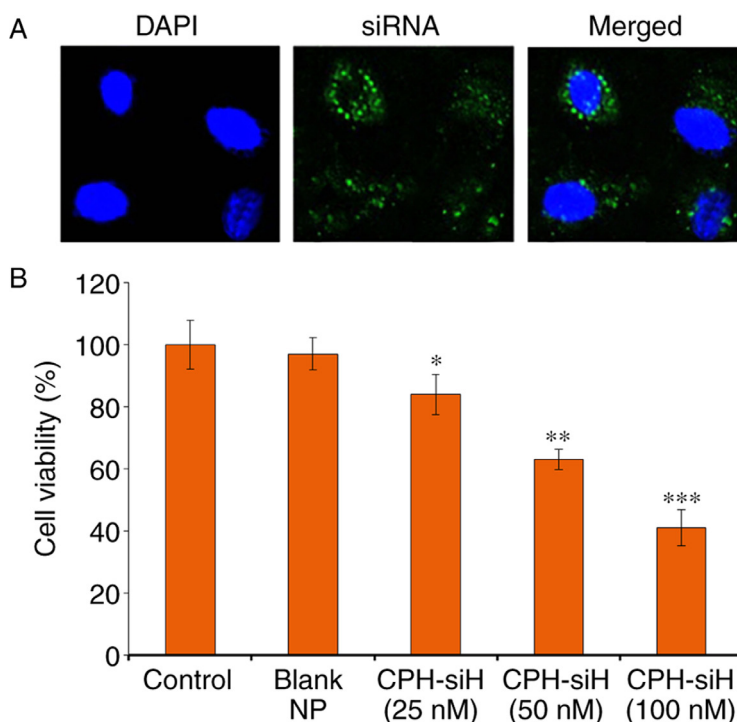
Figure 4. Intracellular distribution and cytotoxicity of the CPH-siH nanoparticles. (A) Cellular internalization of CPH-siH in A549 cells. The lysosome escape property of CPH-siH was evaluated by confocal laser scanning microscopy. Fluorescently-labeled siRNA was used (green), while the nuclei were counterstained with DAPI (blue). (B) Cell viability analysis of A549 cells by MTT assay. The cells were incubated with different concentrations of CPH-siH for 24h. *P<0.05, **P<0.01, ***P<0.001 between control and CPH-siH 100 nm (n=3). CPH-siH, HA-PEI/heparin/Ca^{2+}/siRNA; siRNA, small interfering RNA.

pairwise comparisons. GraphPad Prism, version 17.0 (GraphPad Software, Inc., La Jolla, CA, USA) was for statistical analysis. Data are presented as the mean ± standard deviation. P<0.05 was considered to indicate a statistically significant difference.

Results and discussion

Gene therapy is emerging as an alternative to conventional therapy for cancer, due to its ability to modify gene expression during cancer treatment. In this regard, the oncogene AIB1, which is a member of the p160 steroid receptor coactivator family, was selected as a target in the present study. It was hypothesized that knockdown of the AIB1 gene would result in increased therapeutic efficacy in lung cancer cells. In the present study, a nanocomplex based on PEI/heparin was produced in the presence of Ca^{2+} ions to form intact particles, and to protect the siRNA in the systemic circulation a further protective layer around the PEI/heparin/Ca^{2+} particles was assembled with HA (Fig. 1).

Binding efficiency of AIB1siRNA to CPH-siH NPs. The binding efficiency of siRNA to the CPH-siH was evaluated
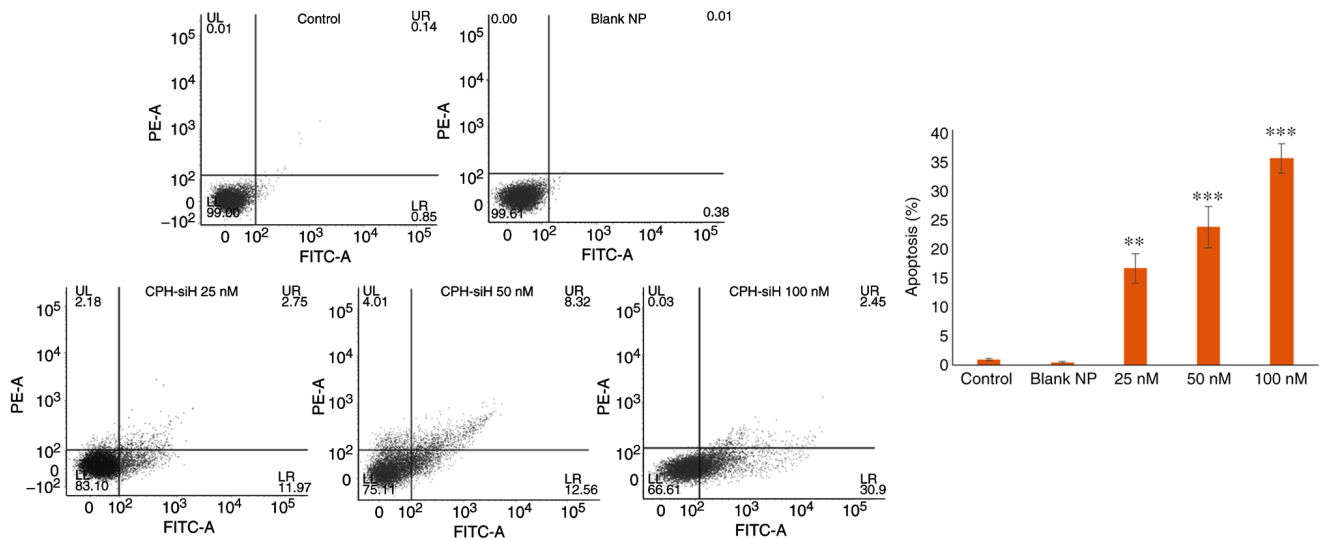
Figure 5. Apoptosis assay of A549 cancer cells following treatment with CPH-siH and blank NPs. The effects of the NPs on cell apoptosis were evaluated by Annexin V-FITC/PI staining and flow cytometry. The histogram was divided into four quadrants for Q1, viable; Q2, necrosis; Q3, early apoptosis, and Q4, late apoptosis, respectively. The graph shows the % of cells in the early and late apoptotic stages relative to the total cell number per sample. CPH-siH, HA-PEI/heparin/Ca^{2+}/siRNA; NPs, nanoparticles; FITC, fluorescein isothiocyanate; PI, propidium iodide. **P<0.01, ***P<0.001 vs. control.
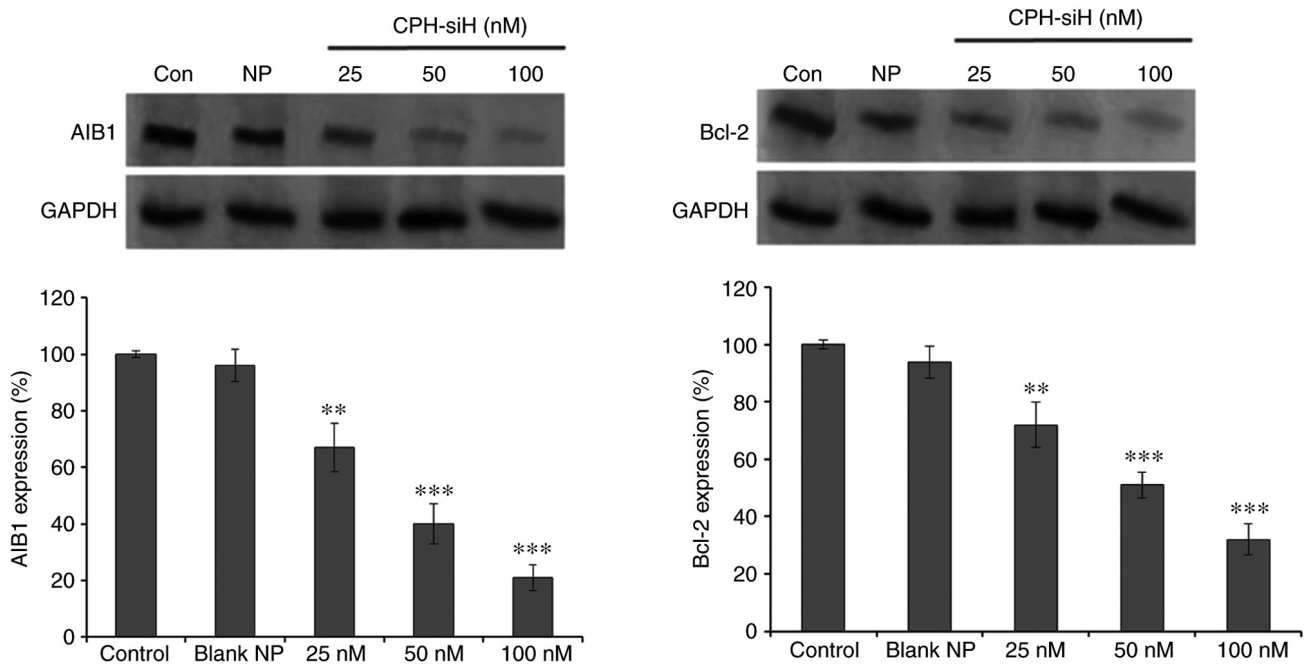
Figure 6. Protein expression levels of AIB1 and Bcl-2 in each treatment group. The knockdown effect of AIB1siRNA-loaded CPH-siH in A549 cancer cells was evaluated by western blotting, using GADPH as a loading control. **P<0.01 and ***P<0.001 compared with control (n=3). AIB1, nuclear receptor coactivator 3; Bcl-2, BCL2 apoptosis regulator; siRNA, small interfering RNA; CPH-siH, HA-PEI/heparin/Ca^{2+}/siRNA; Con, control.

by gel electrophoresis using 2% agarose gels. The ratio of siRNA to CPH-siH was varied from nitrogen/phosphate (N/P) ratios of 1-5. As illustrated in Fig. 2, a marked reduction in the mobility of siRNA was observed with an increase in the N/P ratio; the siRNA band was retained completely when the N/P ratio was 5, indicating its strong binding to the CPH-siH nanoparticles.

Particle characteristics of CPH-siH NPs. The physico-chemical properties of the carrier system affect its fate and efficiency in cancer management. The mean particle size

of PEI/heparin/Ca^{2+}siRNA particles was ~20 nm with a uniform distribution pattern (Fig. 3A). The particle size slightly increased to ~28 nm following coating with HA, indicating that a thin layer of polymer was assembled around the PEI/heparin/Ca^{2+} particles. The HA assembly was further confirmed by the charge reversal pattern. The surface charge of PEI/heparin/Ca^{2+} particles was +22.5±1.26 mV, while it reversed to -18.3±1.42 mV after coating with HA, indicating successful coating. Overall, NPs are expected to increase the delivery of siRNA to the targeted tissues, which may increase the therapeutic efficacy in cancer. The morphology of

CPH-siH was determined by TEM (Fig. 3B). Consistent with the DLS analysis, spherically-shaped nanosized particles were distributed evenly on the copper grid. The nanosized particles coupled with their spherical morphology probably increased the success of the formulation methodology.

Intracellular distribution of CPH-siH. The success of siRNA in cancer cell treatment relies partly in its ability to escape from lysosomal degradation soon after internalization, so as to silence the post-transcriptional gene expression in the cytoplasm (23). To evaluate this property, the internalization pattern of FAM-siRNA was examined. In the microscopic images of Fig. 4A, the cell nucleus was counterstained with DAPI (blue color), and the green color originated from the fluorescently-labeled siRNA. Following 2 h of CPH-siH incubation, most of the fluorescence was observed in the cytoplasm and in the periphery of the nucleus, indicating successful escape from lysosomal degradation and successful internalization of the NPs. It can be concluded that after reaching the lysosomes, FAM-siRNA dissociated from the CPH-siH NPs and exhibited fluorescence in the cytoplasm.

Cytotoxicity of CPH-siH in A549 cancer cells. The cytotoxicity of CPH-siH NPs was evaluated using the MTT assay. The A54p lung cancer cells were treated with different concentrations of CPH-siH NPs and incubated for 24 h. Fig. 4B illustrates that CPH-siH nanoparticles exhibited a typical concentration-dependent toxicity in cancer cells; >60% of cell death was observed when treated with the highest concentration of CPH-siH NPs (siRNA, ~100 nm). Furthermore, blank PEI/heparin/Ca^{2+} NPs did not induce any toxicity in the cancer cells, indicating their safety and lack of side effects (Fig. 4B). It is well-known that PEI induces a cytotoxic effect; however, binding with heparin reduced its toxicity, resulting in biocompatible particles.

Cell apoptosis analysis. To further demonstrate the anticancer effect of AIB1siRNA-loaded CPH-siH NPs, an apoptosis assay using flow cytometry was performed on A549 cancer cells (Fig. 5). The cells were stained with Annexin V and PI as respective viability and apoptosis phase indicators. Consistent with the cell viability assay, the blank NPs did not induce any apoptosis in the cancer cells (Fig. 5). CPH-siH (25 nm) induced ~14% cell apoptosis while the cell apoptosis % increased with the increase in the concentration of siRNA. CPH-siH at 100 nm dose induced the maximum apoptosis of cancer cells, with nearly ~35% of cells in early and late apoptosis stages (Fig. 5), indicating the potent anticancer effect of AIB1siRNA in lung cancer cells.

Protein expression using western blot analysis. The expression levels of the AIB1 protein following treatment with different concentrations of the siRNA-loaded NPs were evaluated by western blot analysis. AIB1 protein was significantly knocked down in a concentration-dependent manner (Fig. 6), indicating the potent activity of AIB1siRNA in cancer cells. The knockdown of AIB1 protein in a concentration-dependent manner was consistent with the cell viability and apoptosis analysis results. The knockdown effect further emphasized the success of transfection and post-transcriptional activity

of the target gene. In addition, the expression levels of the Bcl-2 protein were assessed, and the results demonstrated a concentration-dependent decrease in Bcl-2 protein expression with an increase in the concentration of AIB1siRNA NPs (Fig. 6) (24,25).

Overall, the present study emphasized two important observations. First, AIB1siRNA exhibited a potent anticancer effect in cancer cells, and resulted in the knockdown of the AIB1 gene and a significant cytotoxic effect. Second, PEI/heparin/Ca^{2+}, which did not induce any toxic effects on its own, was demonstrated to be an efficient carrier system for the delivery of a gene into cancer cells. A detailed study on experimental animals to assess the *in situ* and *in vivo* parameters will be the subject of future investigations. Furthermore, further studies combining the NPs with a second therapeutic moiety are warranted.

In conclusion, AIB1siRNA-loaded PEI/heparin/Ca^{2+} NPs were successfully prepared and evaluated for their efficacy in lung cancer cells. The results demonstrated that the PEI and heparin complex reduced the toxic effect in cancer cells while maintaining its transfection efficiency. A nanosized particle of ~25 nm was formulated, and the siRNA was demonstrated to possess excellent binding efficiency in the particles. Confocal microscopy revealed that FAM-siRNA dissociated from the CPH-siH nanoparticles and exhibited maximum fluorescence in the cytoplasm, which is important for its post-transcriptional activity. CPH-siH NPs exhibited a typical concentration-dependent toxicity in cancer cells, while blank PEI/heparin/Ca^{2+} did not induce any toxicity, indicating its safety and lack of side effects. CPH-siH at the dose of 100 nm induced the maximum apoptosis of cancer cells with ~35% of cells in the early and late apoptosis stages. The AIB1 protein was knocked down in a concentration-dependent manner, demonstrating the potent activity of AIB1siRNA in cancer cells. Together, these findings indicated that PEI/heparin/Ca^{2+}-HA NPs may be promising carriers for the anticancer activity of AIB1siRNA in lung cancer cells.

Availability of data and materials

The analyzed datasets generated during the study are available from the corresponding author on reasonable request.

Authors' contributions

YW and YH were actively involved in all *in vitro* biological assays and preparation protocols. YG secured the internal research grant and was associated with the design and writing the manuscript. CA was involved in writing and proofreading the entire manuscript with experimental insight. All authors read and approved the final manuscript.

Ethics approval and consent to participate

Not applicable.

Patient consent for publication

Not applicable.

Competing interests

The authors declare that they have no competing interests.

References

1. Gomes Neto A, Simão AFL, Miranda Sde P, Mourão LT, Bezerra NP, Almeida PR and Ribeiro Rde A: Experimental rat lung tumor model with intrabronchial tumor cell implantation. Acta Cir Bras 23: 84-92, 2008.
2. Molina JR, Yang P, Cassivi SD, Schild SE and Adjei AA: Non-small cell lung cancer: Epidemiology, risk factors, treatment, and survivorship. Mayo Clin Proc 83: 584-594, 2008.
3. Sun S, Schiller JH and Gazdar AF: Lung cancer in never smokers-a different disease. Nat Rev Cancer 7: 778-790, 2007.
4. Ettinger DS, Akerley W, Bepler G, Blum MG, Chang A, Cheney RT, Chirieac LR, D'Amico TA, Demmy TL, Ganti AK, et al: Non-small cell lung cancer. J Natl Compr Cancer Network 8: 740-801, 2010.
5. Goldstraw P, Ball D, Jett JR, Le Chevalier T, Lim E, Nicholson AG and Shepherd FA: Non-small-cell lung cancer. Lancet 378: 1727-1740, 2011.
6. Wolinsky JB, Colson YL and Grinstaff MW: Local drug delivery strategies for cancer treatment: Gels, nanoparticles, polymeric films, rods, and wafers. J Control Release 159: 14-26, 2012.
7. Ramasamy T, Ruttala HB, Gupta B, Poudel BK, Choi HG, Yong CS and Kim JO: Smart chemistry-based nanosized drug delivery systems for systemic applications: A comprehensive review. J Control Release 258: 226-253, 2017.
8. Sokolova V and Epple M: Inorganic nanoparticles as carriers of nucleic acids into cells. Angew Chem Int Ed Engl 47: 1382-1395, 2008.
9. Sun TM, Du JZ, Yao YD, Mao CQ, Dou S, Huang SY, Zhang PZ, Leong KW, Song EW and Wang J: Simultaneous delivery of siRNA and paclitaxel via a 'two-in-one' micelleplex promotes synergistic tumor suppression. ACS Nano 5: 1483-1494, 2011.
10. Henke RT, Haddad BR, Kim SE, Rone JD, Mani A, Jessup JM, Wellstein A, Maitra A and Riegel AT: Overexpression of the nuclear receptor coactivator AIB1 (SRC-3) during progression of pancreatic adenocarcinoma. Clin Cancer Res 10: 6134-6142, 2004.
11. Liu MZ, Xie D, Mai SJ, Tong ZT, Shao JY, Fu YS, Xia WJ, Kung HF, Guan XY and Zeng YX: Overexpression of AIB1 in nasopharyngeal carcinomas correlates closely with advanced tumor stage. Am J Clin Pathol 129: 728-734, 2008.
12. Kuang SQ, Liao L, Zhang H, Lee AV, O'Malley BW and Xu J: AIB1/SRC-3 deficiency affects insulin-like growth factor I signaling pathway and suppresses v-Haras-induced breast cancer initiation and progression in mice. Cancer Res 64: 1875-1885, 2004.
13. Xu JM, Liao L, Ning C, Yoshida-Komiya H, Deng C and O'Malley BW: The steroid receptor coactivator SRC-3 (p/CIP/RAC3/AIB1/ACTR/TRAM-1) is required for normal growth, puberty, female reproductive function, and mammary gland development. Proc Natl Acad Sci USA 97: 6379-6384, 2000.
14. Ruttala HB, Ramasamy T, Madeshwaran T, Hiep TT, Kandasamy U, Oh KT, Choi HG, Yong CS and Kim JO: Emerging potential of stimulus-responsive nanosized anticancer drug delivery systems for systemic applications. Arch Pharm Res 41: 111-129, 2018.
15. Gautam A, Densmore CL, Golunski E, Xu B and Waldrep JC: Transgene expression in mouse airway epithelium by aerosol gene therapy with PEI-DNA complexes. Mol Ther 3: 551-556, 2001.
16. Godbey WT, Wu KK and Mikos AG: Poly(ethylenimine) and its role in gene delivery. J Control Release 60: 149-160, 1999.
17. Goula D, Benoist C, Mantero S, Merlo G, Levi G and Demeneix BA: Polyethylenimine-based intravenous delivery of transgenes to mouse lung. Gene Ther 5: 1291-1295, 1998.
18. Lehman CM and Frank EL: Laboratory monitoring of heparin therapy: Partial thromboplastin time or anti-Xa assay? Lab Med 40: 47-51, 2009.
19. Josephson L, Tung CH, Moore A and Weissleder R: High-efficiency intracellular magnetic labeling with novel superparamagnetic-Tat peptide conjugates. Bioconjug Chem 10: 186-191, 1999.
20. Scheicher B, Schachner-Nedherer AL and Zimmer A: Protamine-oligonucleotide-nanoparticles: Recent advances in drug delivery and drug targeting. Eur J Pharm Sci 75: 54-59, 2015.
21. Yang X, Du H, Liu J and Zhai G: Advanced nanocarriers based on heparin and its derivatives for cancer management. Biomacromolecules 16: 423-436, 2015.
22. Ramasamy T, Tran TH, Choi JY, Cho HJ, Kim JH, Yong CS, Choi HG and Kim JO: Layer-by-layer coated lipid-polymer hybrid nanoparticles designed for use in anticancer drug delivery. Carbohydr Polym 102: 653-661, 2014.
23. Ma G, Ren Y, Wang K and He JJ: SRC-3 has a role in cancer other than as a nuclear receptor coactivator. Int J Biol Sci 7: 664-672, 2011.
24. Colo GP, Rosato RR, Grant S and Costas MA: RAC3 down-regulation sensitizes human chronic myeloid leukemia cells to TRAIL-induced apoptosis. FEBS Lett 581: 5075-5081, 2007.
25. Sundaramoorthy P, Ramasamy T, Mishra SK, Jeong KY, Yong CS, Kim JO and Kim HM: Engineering of caveolae-specific self-micellizing anticancer lipid nanoparticles to enhance the chemotherapeutic efficacy of oxaliplatin in colorectal cancer cells. Acta Biomater 42: 220-231, 2016.